Discovery of Enhanced Nuclear Stability near the Deformed Shells $N = 162$ and $Z = 108$

Yu. A. Lazarev, Yu. V. Lobanov, Yu. Ts. Oganessian, V. K. Utyonkov, F. Sh. Abdullin, G. V. Buklanov, B. N. Gikal, S. Iliev, A. N. Mezentsev, A. N. Polyakov, I. M. Sedykh, I. V. Shirokovsky, V. G. Subbotin, A. M. Sukhov, Yu. S. Tsyganov, and V. E. Zhuchko
Joint Institute for Nuclear Research, 141980 Dubna, Russia

R. W. Lougheed, K. J. Moody, J. F. Wild, E. K. Hulet, and J. H. McQuaid
University of California, Lawrence Livermore National Laboratory, Livermore, California 94551
(Received 31 March 1994)

In bombardments of ^{248}Cm with ^{22}Ne we discovered two new isotopes, ^{265}106 and ^{266}106, by establishing genetic links between their α decays and spontaneous fussion (SF) or α decays of the daughter nuclides. We measured $E_\alpha = 8.63 \pm 0.05$ MeV for ^{266}106 and a half-life of 1.2 s for its daughter ^{262}104. For ^{265}106 we measured $E_\alpha = 8.71$ to 8.91 MeV. From these α energies we estimated α half-lives of 10–30 s for ^{266}106 and 2–30 s for ^{265}106. We estimated SF branches of 50% or less for both isotopes. The decay properties of ^{266}106 establish the existence of enhanced nuclear stability near the predicted deformed shells $N = 162$ and $Z = 108$.

PACS numbers: 21.10.Tg, 23.60.+e, 25.70.Gh, 27.90.+b

Recent macroscopic-microscopic calculations (see, e.g., Refs. [1–5]) all show an especially large negative shell correction for the ground states of nuclei at and near $N = 162$ and $Z = 108$ due to a large gap in the Nilsson levels between $N = 162$ and 163 and $Z = 108$ and 109, which is further enhanced by considering higher order multipolarities of deformed shapes, particularly the hexadecapole vibration. However, spontaneous fission (SF) is usually the limiting decay mode for even-even nuclides in this region and estimations of SF half-lives from barrier penetration probabilities vary by many orders of magnitude. Although the calculated static barrier heights are about equal, differences in half-life estimates can be attributed to differing assumptions regarding the dynamical path through the fission barrier and the consequent inertial mass. For example, Möller and co-workers [5], taking ^{258}Fm as a model for heavier nuclei, assume that the path after the first barrier is short with the emerging fragments being nearly spherical and close to the doubly magic ^{132}Sn. On the other hand, Patyk, and co-workers [2–4] calculate dynamical barriers that show a different path, higher inertial mass, and consequently much longer SF half-lives. This competition between static and dynamic features of the SF process which lead to such large differences in stability makes experiments that explore ground-state decay properties of nuclei around $N = 162$ and $Z = 108$ one of the most important tasks in heavy element research.

We report here on our experiments resulting in the first direct evidence of nuclear stability near both the predicted deformed shells by producing the even-even $N = 160$ nuclide ^{266}106 (and also ^{265}106). The only previously known nuclide with $N = 160$, the 5 ms isotope ^{262}102, provided a hint of unexpected stability against SF [6]. Prior to our work, four isotopes of element 106 had been identified. These are the odd-A α emitters ^{259}106 [7], ^{261}106 [7], and ^{263}106 [8], with half-lives in the range of 0.3 to 0.9 s, and the 3.6 ms even-even isotope ^{260}106 [7, 9, 10] which has a SF branch of $50^{+30}_{-20}\%$.

The ground-state decay properties of ^{266}106 should be a quite sensitive probe of the theoretical predictions shown in Fig. 1. If there is increased stability near $N = 162$ and $Z = 108$, the isotope ^{266}106 should have a SF or α decay half-life of tens of seconds. Otherwise, ^{266}106 should decay by SF with a half-life of ~ 100 μs, a T_{SF} difference of $\sim 10^5$ (see Fig. 1). Thus a distinct signature for enhanced nuclear stability near $N = 162$ and $Z = 108$ would be the observation of the α decay of ^{266}106 followed by the SF decay of the daughter nucleus ^{262}104.

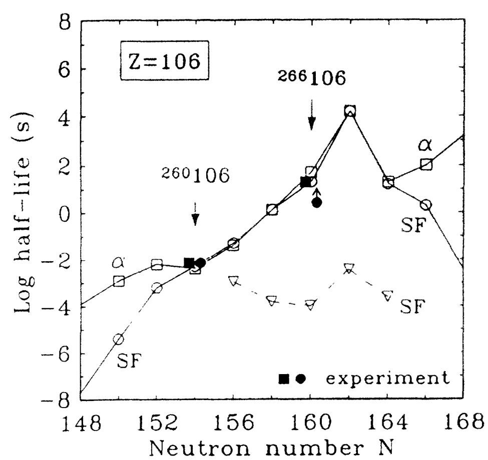

FIG. 1. Predicted partial half-lives [4] for SF and α decay of the even-even 106 isotopes shown by the lines connecting circles and squares, respectively. The dashed line connecting the triangular points shows SF half-life predictions [5]. The experimental values for ^{260}106 [7,10] and the results for ^{266}106 from this work are shown for comparison.

0031-9007/94/73(5)/624(4)$06.00

A signature for the odd-A isotope $^{265}106$ would be the observation of its α decay followed by α decays of the known nuclides $^{261}104$ and $^{257}102$.

To produce $^{265}106$ and $^{266}106$ we used the complete fusion reaction ^{248}Cm + ^{22}Ne at bombarding energies of 116 and 121 MeV which are expected to provide maximum cross sections for the $4n$ and $5n$ evaporation channels. Beams of ^{22}Ne projectiles from U400 cyclotron of the Joint Institute for Nuclear Research passed through rotating 3-μm Ti foils and curium targets (97% ^{248}Cm and 3% ^{246}Cm). Three targets with average areal densities of 240 μg cm^{-2} of ^{248}Cm and a total area of 11.7 cm^2 were arranged on a wheel whose rotation was synchronized to the 150 Hz frequency of the cyclotron so that a target was exposed to the ~2 ms beam macropulse during 6.7 ms beam cycle. The targets were electrodeposited on 710 μg cm^{-2} Ti foils and covered by a 30 μg cm^{-2} carbon layer. The targets received a total beam dose of about 1.6×10^{19} particles with typical intensities of 1.3×10^{13} particles/s of ^{22}Ne.

Evaporation residues (EVRs) recoiling out of the ^{248}Cm targets were separated in-flight from beam particles and transfer products by the Dubna gas-filled recoil separator described in Ref. [11]. The separator was filled with hydrogen at a pressure of 0.7 Torr. We set the magnetic rigidity of the separator's dipole magnet for the slow $Z = 106$ EVRs according to prior measurements [11] of the average charge state in hydrogen, $\langle q \rangle$, for the slow EVRs with $Z = 100$, 102, and 104 produced in the reactions ^{235}U + ^{18}O, ^{235}U + ^{22}Ne, and ^{242}Pu + ^{22}Ne. The separated EVRs passed through a time-of-flight (TOF) measurement system composed of two multiwire proportional chambers in a 1 Torr pentane-filled module and were finally implanted in a position-sensitive surface-barrier detector (PSD) array.

The PSD array consisted of three surface-barrier detectors, with each detector having eight 40 mm high × 4.8 mm wide strips. We obtained horizontal positions for the reaction products from 24 strips and vertical positions from 40 mm high resistive back of the detectors. A particle striking a detector generated a signal in a strip and in the resistive back of the detector. Signals from the detector strips were processed for α and implant energies. Top and bottom signals from the back of each detector were split into two channels to provide position signals in the 40 mm direction for α/implant events (~0.5 to 15 MeV) and fission events (15 to 200 MeV). We calculated total fission energies by summing the position energy signals. With each detected event, we also recorded the strip number, TOF information, beam current, the time in μs from the beginning of each beam pulse to either α/implant or fission events, and the time since the beginning of the data acquisition cycle in 0.1 ms intervals. The data were accumulated in list mode in a LSI 11/73 computer and periodically transferred to a microVAX computer for storage and off-line analysis.

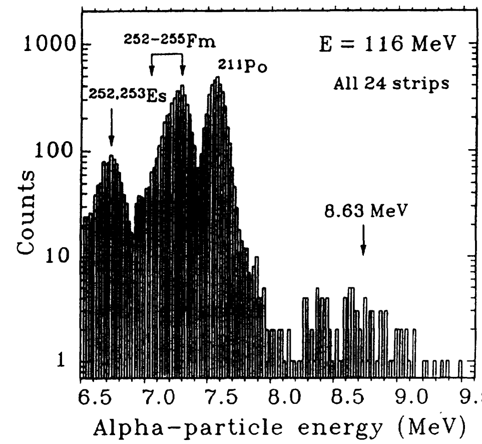

FIG. 2. Out-of-beam α-energy spectrum from all detectors at 116 MeV (1.0×10^{19} particles ^{22}Ne). The spectrum at 121 MeV (0.6×10^{19} particles ^{22}Ne) is very similar.

Alpha-energy calibrations were performed for each strip using the α peaks from nuclides produced in the ^{197}Au + ^{22}Ne reaction. Most of the strips had energy resolutions of about 100 keV. An approximate fission-energy calibration was obtained by extrapolating the α-energy calibration and by setting the separator magnetic rigidity so that ^{22}Ne projectiles of known energy impinged upon the detectors. We also performed a calibration bombardment of ^{235}U with 1.3×10^{18} particles of ^{22}Ne to measure the α and SF activities from the known nuclide $^{252}102$ and to estimate the EVR collection efficiency. We used known α-α, EVR-α, and EVR-SF sequences from the calibration reactions to estimate FWHM position resolutions of ~3% of the strip length for the α-α sequences and ~9% for α-SF or EVR-α sequences.

We had low efficiencies for detecting EVRs because the initial $Z = 106$ EVR energy of 7 MeV was reduced to ~2 MeV implantation energy due to losses in the target, hydrogen gas, and the TOF module. The measured energy was expected to be about half the implantation energy mainly due to plasma effects and losses in the detector dead layer. This resulted in most of the EVR signals being below the detection threshold.

In the off-line analyses we searched for time and position correlated α-SF and α-α event chains. We list in Table I the observed α-SF and α-α-(α) correlations. The out-of-beam counting rate for α's in the energy range of interest (Fig. 2) and for SF events (Fig. 3) was extremely low, ~1 event per day per strip regardless of the bombarding energy, providing a very high statistical significance for all the correlations in Table I. Using our data we calculated the probabilities that the four out-of-beam α-SF correlations and the two α-SF correlations with the α in-beam are of random origin are less than $10^{-15}$and less than 10^{-4}, respectively.

We attribute the six α-SF event pairs at 116 and 121 MeV with a maximum likelihood result of $E_\alpha =$

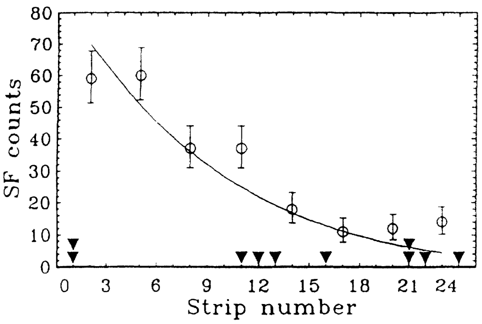

FIG. 3. The distribution of all detected 248 out-of-beam events at 116 MeV (open circles). Events from each three adjacent strips are summed. The distribution at 121 MeV is very similar. The curve is a least-squares fit to a Gaussian distribution across the detector strips for the Fm α events shown in Fig 2; the curve is normalized to the measured α/SF ratio. The triangles show the location of the α/SF and α-α-(α) correlations from both the 116 and 121 MeV bombardments.

TABLE I. The measured parameters of the α-SF and α-α correlation chains observed in the ^{248}Cm + ^{22}Ne reaction. All events are out-of-beam except for those three indicated.

Decay mode	Particle energy, MeV[a]	Strip number	Time interval	Δ pos., mm
		116 MeV		
α	8.60	16		
SF	105	16	191 ms	3.0
α	8.54	22		
SF	89	22	215 ms	3.0
α	8.59	24		
SF	96	24	748 ms	1.3
α	8.74	21		
SF	118	21	6453 ms	1.8
		121 MeV		
α[b]	8.69	11		
SF[b]	103	11	360 ms	0.3
α[b]	8.60	13		
SF	118	13	2011 ms	1.8
α	8.85	21		
α	8.20	21	3 s	0.8
α	8.81	1		
α	8.31	1	334 s	0.3
α	8.17	1	60 s	1.0
α[c]	8.91	1		
α	8.12	1	86 s	?
α	8.71	12		
α	8.14	12	20 s	0.2
α	8.16	8		
α	8.17	8	1 s	0.7

[a]The quoted fission fragment energies are measured values. No estimate was included for the pulse-height defect or the fraction of the total kinetic energy deposited in the detectors.
[b]Event occurred during the beam pulse.
[c]Position signals were not detected for this event.

8.63 ± 0.05 MeV to the decay chain $^{266}106 \Rightarrow {}^{262}104$ for which we measured a production cross section of 80 pb at 116 MeV and 60 pb at 121 MeV. We assigned the four α-α-(α) correlations at 121 MeV with $E_{\alpha 1}$ = 8.71 to 8.91 MeV to the decay chain $^{265}106 \Rightarrow {}^{261}104$ ($T_{1/2}$ = 65 s, $E_\alpha \sim 8.29$ MeV) $\Rightarrow {}^{257}102$ ($T_{1/2}$ = 26 s, $E_\alpha \sim$ 8.22, 8.27, 8.32 MeV) for which we measured a production cross section of 260 pb. The cross sections are reported with an estimated accuracy of a factor of ~3. We attribute the 8.16 to 8.17 MeV α-α correlation to the decay chain $^{261}104 \Rightarrow {}^{257}102$. We note that except for the triple correlation, one cannot distinguish between $^{261}104$ and $^{257}102$ due to their similar α energies and half-lives.

Our assignment of the six α-SF correlations to the decay of $^{266}106$ is based on the following observations. The α-SF correlation chains with E_α = 8.63 MeV and short time intervals from 0.2 to 6.5 s are unique; for the synthesis reaction that we employed, one cannot identify any candidate α-SF decay sequences with other Z,A values which would have similar decay properties. Furthermore, the 8.63 MeV α energy is in agreement with both predictions and systematics [3,4] as is the SF decay mode for the Z = 104 daughter. The six α-SF correlation chains were detected by using the gas-filled recoil separator which strongly suppresses beam particles and many kinds of background reaction products relative to compound nucleus products. The α-SF and α-α chains were broadly distributed across the detector array as expected for products of the (^{22}Ne,4–5n) reactions, while the largest number of single SF and α events, which come from transfer products like ^{256}Fm and lighter Fm isotopes, occurred closer to the end of the detector array that corresponds to lower magnetic rigidity values (Fig. 3). From our data, we estimated the average charge state $\langle q \rangle$ of the slow $Z=106$ EVRs in hydrogen to be $2.0^{+0.2}_{-0.3}$ at $\langle v/v_0 \rangle \approx 1.0$ ($v_0 = 2.2 \times 10^6$ m s^{-1} is the Bohr velocity), in full agreement with the previous $\langle q \rangle$ measurements [11] for Z = 100–104. Finally, the production cross sections for the α-SF correlations at both 116 and 121 MeV agree with systematics.

We assigned the four α-α correlations with $E_{\alpha 1}$ = 8.71 to 8.91 MeV to the decay of $^{265}106$ using arguments similar to those given above for $^{266}106$. Especially convincing is the triple-α correlation.

The above observations and arguments provide consistent evidence for the assignment of the correlation chains to the α decay of $^{265}106$ and $^{266}106$. The correlation times for the six α-SF chains give a half-life of $1.2^{+1.0}_{-0.5}$ s for $^{262}104$. A SF activity with $T_{1/2} \sim 47$ ms was tentatively assigned by Somerville *et al.* [12] to $^{262}104$. In fact, an unassigned 1.3 s SF activity was also produced at the near-barrier bombarding energies 89 and 95 MeV in the ^{248}Cm + ^{18}O reaction [12]. Moreover, Hoffman *et al.* [13] produced a 1.5 s SF activity and measured its fission properties in the same ^{248}Cm + ^{18}O reaction at

95 MeV. Since the alpha decay of even-even nuclides is ground state to ground state our findings establish that the total half-life of the ground state decay of $^{262}104$ is 1.2 s.

We estimated the partial α-decay half-lives of $^{265,266}106$ from the measured α-decay energies. For the even-even nuclide $^{266}106$ this estimation is straightforward. Using the phenomenological formula of Viola and Seaborg in Ref. [3], we determined a partial α half-life for $^{266}106$ of 10 to 30 s. Similarly, we obtained an α half-life of 2 to 30 s for $^{265}106$ assuming a hindrance factor between 1 and 3.

The α-branching ratios are probably $\geq 50\%$ for both 106 nuclides based on our cross-section evaluations which are about the expected values for the $4n$ and $5n$ evaporation channels. We set a very conservative α-branching lower limit of 15% for $^{266}106$ from the beam-off data at 116 MeV by assuming that *all* of the observed fissions detected in strips numbered 16 to 24 (Fig. 3) are from SF decay of $^{266}106$ or its daughter, $^{262}104$. Most of the observed SF events are actually from the transfer product ^{265}Fm, based on their distribution across the strips and on their yield compared to that of α-emitting Fm isotopes [14].

The ground-state decay properties that we established for $^{266}106$ reveal a significantly increased stability near $N = 162$ and $Z = 108$ and are in agreement with the theoretical predictions made in Refs. [1–4]. The half-life of 1.2 s for $^{262}104$ also signals the trend toward greater nuclear stability with N approaching 162. The short SF half-lives predicted by Möller and co-workers [5] are inconsistent with our results.

The enhanced nuclear stability near $N = 162$ and $Z = 108$ discovered in the present work can be compared with the enormous influence of the $N = 152$ deformed shell on SF half-lives and creates new opportunities for many further explorations at the edge of the nuclear domain.

We thank the U400 cyclotron staff for providing long-term bombardments with intense ^{22}Ne beams. We thank V. V. Bekhterev, I. V. Kolesov, V. I. Krashonkin, the late V. M. Plotko, L. I. Salamatin, D. H. Tinoco, J. T. Walton, and E. D. Watkins for their essential help. Part of the curium target material was provided by the OBES, U.S. DOE, through ORNL. Most of the support of the Livermore collaborators was provided through the U.S. DOE by the Lawrence Livermore National Laboratory under Contract No. W-7405-Eng-48. These studies were performed in the framework of the U.S./Russian Federation Joint Coordinating Committee for Research on Fundamental Properties of Matter.

[1] S. Čwiok *et al.*, Nucl. Phys **A410**, 254 (1983).
[2] Z. Patyk *et al.*, Nucl. Phys. **A502**, 591c (1989).
[3] Z. Patyk and A. Sobiczewski, Nucl. Phys. **A533**, 132 (1991).
[4] A. Sobiczewski, in Proceedings of the Actinides-93 Conference, 19–24 September 1993, Santa Fe, NM (to be published).
[5] P. Möller, J.R. Nix, and W.J. Swiatecki, Nucl. Phys. **A469**, 1 (1987); **A492**, 349 (1989); P. Möller and J.R. Nix, Nucl. Phys. **A549**, 84 (1992).
[6] R.W. Lougheed *et al.*, *Fifty Years with Nuclear Fission* (American Nuclear Society, La Grange Park, IL, 1989) Vol. 2, p. 694.
[7] G. Münzenberg *et al.*, Z. Phys. A **322**, 227 (1985).
[8] A. Ghiorso *et al.*, Phys. Rev. Lett. **33**, 1490 (1974).
[9] Yu. Ts. Oganessian *et al.*, Pis'ma Zh. Eksp. Teor. Fiz. **20**, 580 (1974) [JETP Lett. **20**, 265 (1974)].
[10] A. G. Demin *et al.*, Z. Phys. A **315**, 197 (1984).
[11] Yu. A. Lazarev *et al.*, in *Heavy Ion Physics, Scientific Report 1991-1992* (JINR Report No. E7-93-57, Dubna, 1993), p. 203; in *Proceedings of the International School Seminar on Heavy Ion Physics, Dubna, 1993* (JINR Report No. E7-93-274, Dubna, 1993), Vol. 2, p. 497.
[12] L. P. Somerville *et al.*, Phys. Rev. C **31**, 1801 (1985); L. P. Somerville, Ph.D. thesis, University of California [Report No. LBL-14050, Berkeley, 1982].
[13] D. C. Hoffman *et al.*, Phys. Rev. C **24**, 495 (1981).
[14] D. Lee *et al.*, Phys. Rev. C **25**, 286 (1982).

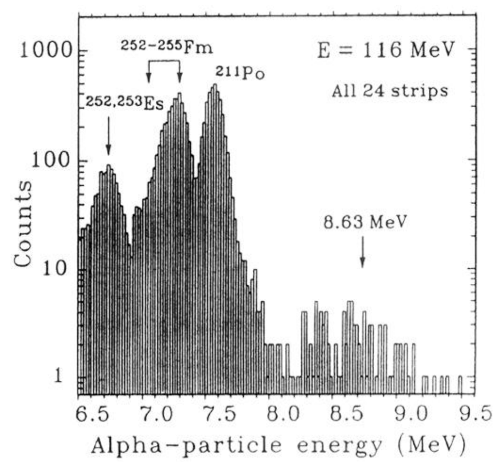

FIG. 2. Out-of-beam α-energy spectrum from all detectors at 116 MeV (1.0×10^{19} particles ^{22}Ne). The spectrum at 121 MeV (0.6×10^{19} particles ^{22}Ne) is very similar.